

Acoustic surface-wave study of magnetoelastic effects in a thin film of $\text{YBa}_2\text{Cu}_3\text{O}_7$

R. Höhler, J. Joffrin, and J. Y. Prieur

Université Paris-Sud, Laboratoire de Physique des Solides, Bâtiment 510, F-91405 Orsay, France

R. Wördenweber and J. Schneider

Institut für Schicht und Ionentechnik, Forschungszentrum Jülich, D-5170 Jülich, Germany

(Received 29 December 1992; revised manuscript received 8 April 1993)

We have measured the velocity of Rayleigh waves in a thin film of $\text{YBa}_2\text{Cu}_3\text{O}_7$ at low temperatures in the presence of a magnetic field of 7 T. The angle between the c axis and the field direction was continuously varied by 180° inside the cryostat at fixed temperatures. Below the superconducting transition temperature the data show a sharp peak for a direction of the applied field that is perpendicular to the c axis. We explain this phenomenon quantitatively as an effect of the anisotropy of the effective electronic mass.

INTRODUCTION

In the recent literature, quite a number of acoustic investigations of high- T_c superconductors have been reported. However, many of them do not give any results that are directly related to superconductivity. The situation is more favorable for experiments in a magnetic field. Vibrating reed¹ and more recently ultrasonic bulk wave measurements² have been used to detect characteristic anomalies that are due to vortex pinning. A major problem of the ultrasonic experiments is the insufficient size and quality of the high- T_c superconductor monocrystals that are available. Therefore several investigators have performed surface acoustic wave measurements on thin film samples.³⁻⁵ One of them⁵ tried to detect magnetoelastic attenuation effects but did not find any within his experimental resolution.

In the following paper we will show that with an improved measurement technique it is possible to detect a magnetoelastic anomaly of $\text{YBa}_2\text{Cu}_3\text{O}_7$ which is due to properties of the vortex lattice. One can take advantage of the strong anisotropy of the effect by measuring the velocity of surface waves in a thin film sample that is slowly rotated in the presence of a strong magnetic field at fixed temperatures. Since to our knowledge no theoretical analysis of magnetoelastic surface-wave effects in thin films has been published in the literature we present a general theory of the physical effects that can be observed by our experiment. We show that a straightforward calculation of the Rayleigh wave properties with magnetoelastic bulk wave corrections applied to the elastic constants of the thin film would lead to wrong results. The dominant effects are due to an oscillating electromagnetic stray field that is induced by the elastic wave. Its lateral extent is independent of the layer thickness, it is roughly given by the acoustic wavelength divided by π . This field perturbation leads to forces that act on the layer and thereby modify the sound velocity.

Surface acoustic waves in the presence of a strong magnetic field are thus a sensitive tool for measuring electromagnetic properties of thin films. We will show in this

paper that in the case of superconductors this method can be used to obtain the anisotropy of the effective electronic mass and parameters which characterize the pinning of vortices at low temperatures.

EXPERIMENT

Since acoustic surface waves are most easily generated and detected on the surface of piezoelectric crystals we have chosen Y-cut LiNbO_3 as a substrate. Conventional techniques for depositing $\text{YBa}_2\text{Cu}_3\text{O}_7$ do not work well on this material: diffusion and interface reactions during the deposition are a major problem.⁶ However, good results can be obtained by a particular dc magnetron sputtering procedure.⁷ The newly deposited films whose thickness was 300 nm had a midpoint of the resistive transition of 89 K, the width was 2 K. We have patterned the films into a rectangular bar of $1 \times 8 \text{ mm}^2$ along the z axis of the substrate and a $10\text{-}\mu\text{m}$ -wide line with four contacts for resistance measurements immediately next to it. On both sides of the bar we have deposited interdigital surface-wave transducers with a fundamental frequency of 100 MHz. After these lithographic processes the critical temperature was somewhat reduced: the midpoint was at 87 K and a small "foot" of the resistance curve extended down to 84 K. The growth direction of the film is unusual: the c axis is strongly tilted with respect to the surface normal. This orientation turned out to be very useful for distinguishing between intrinsic effects that are symmetric with respect to the c axis and effects due to the boundary geometry which are symmetric to the surface normal. A comparison of the values obtained for the tilt angle by these symmetry arguments with pole figure data will be given in the following section. The measurements were performed in a cryostat whose sample holder is placed in the field of a 7-T superconducting magnet and can be turned by 200° at low temperatures. The measurement of the Rayleigh wave velocity was carried out at 100, 300, and 500 MHz by a standard phase-locked loop technique. At 4 K and for fixed angles and fields the measured velocity varied by less

than 1 ppm on the time scale of a typical angular sweep. At 100 K the stability was somewhat reduced because due to the well-known phonon anharmonicity effects the sound velocity varies much more with temperature in that case. In order to check possible phase changes due to the deformation of the high-frequency cables that lead to the sample holder we have performed angular sweeps at fixed temperatures above the superconducting transition. No significant phase change was observed. The absolute value of the magnetoelastic anomaly, that is, the vertical offset of the curves presented in the following section, is not very precise. The uncertainty of the magnetoelastic resistance of the carbon glass resistors we used for measuring the sample temperature corresponds to a shift of the sound velocity of up to 5 ppm.

EXPERIMENTAL RESULTS

At 81 K and at higher temperatures the total angular variation of the Rayleigh wave velocity in a field of 7 T was less than 2 ppm in the entire investigated frequency range.

At 76 K we have observed a sharp peak as can be seen in Fig. 1. Zero field cooled and field cooled data did not show any significant differences, neither did we detect any angular hysteresis effects. The peak amplitude rapidly increases with falling temperature as can be seen in Fig. 2. Below about 69 K a qualitatively new angular behavior sets in: this rapidly increasing contribution is in a good approximation proportional to the square of the cosine of the angle between the applied field and the film surface. Figure 3 shows that it is dominant at 5 K. It is interesting to note that the angular sound velocity anomaly at low temperatures is symmetric to the surface normal whereas the effect at temperatures close to T_c is symmetric with respect to a direction that is 25° – 30° different. We could not determine this angle more precisely because our sample holder was not designed for accurate measurements of absolute directions. The presence of the tilt angle made us think that the c axis of the sample may be tilted with respect to the surface normal.

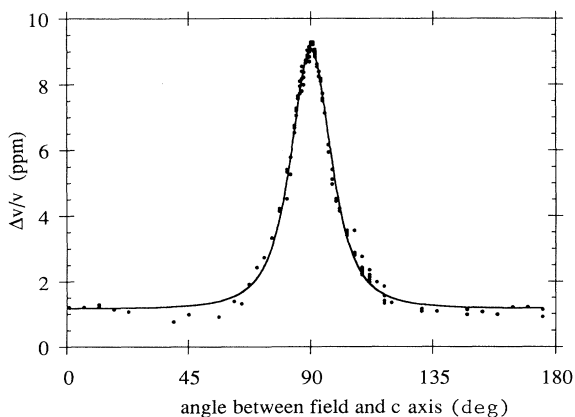


FIG. 1. Sound velocity anomaly at 100 MHz and in a field of 7 T at a fixed temperature of 76 K. The fitted curve is explained in the text.

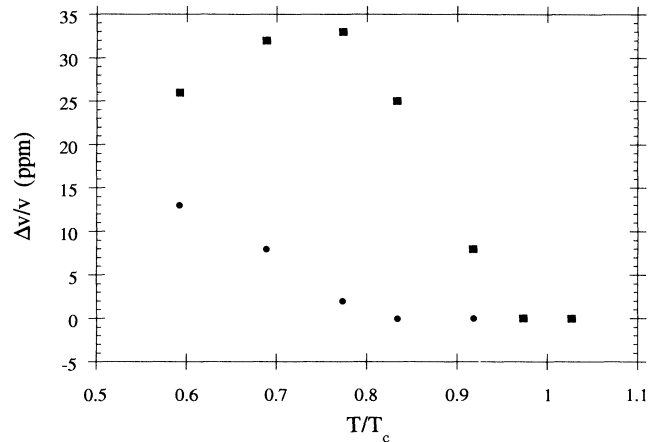


FIG. 2. Peak amplitude of the sound velocity anomaly as a function of reduced temperature. The circles and the squares correspond to a decomposition into contributions whose angular variations are symmetric with respect to the surface normal and to the c axis. The frequency is 100 MHz, the field strength is 7 T.

This hypothesis was confirmed by a pole figure measurement which turned out to be compatible with a tilt angle of 35° . This is somewhat larger than the value that we estimated on the basis of the ultrasonic data; the difference is probably due to the above-mentioned experimental problem.

Figure 2 shows that at the onset temperature of the second effect the first abruptly stops increasing and eventually diminishes at still lower temperatures. For the separation of the two components at intermediate temperatures the above-mentioned symmetry criterion was used.

Close to the superconducting transition the sound velocity variations measured at different temperatures essentially differ by global scale factors. This can be seen in Fig. 4 which shows a masterplot of sound velocity data measured at 69 and 74 K at a frequency of 500 MHz. At lower temperatures there are rapidly increasing devia-

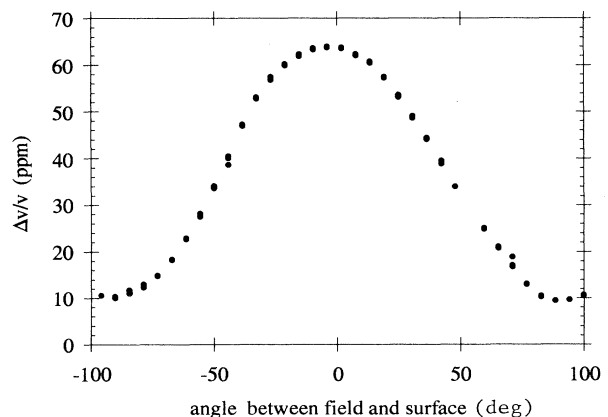


FIG. 3. Rayleigh wave velocity as a function of the angle between the surface tangent and an applied magnetic field of 7 T. The frequency is 100 MHz, the temperature is 5 K.

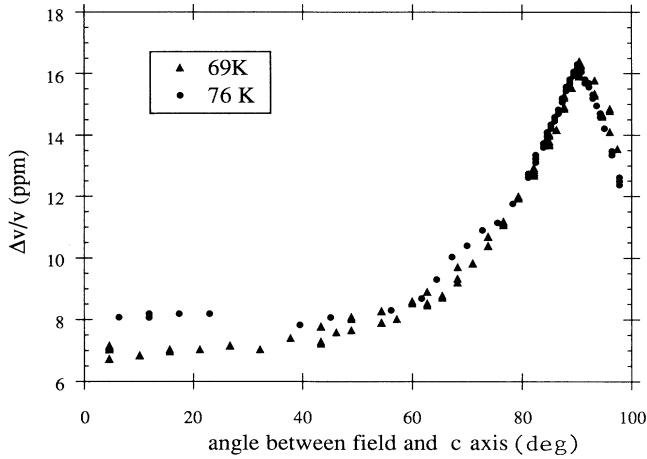


FIG. 4. This plot shows that the shape of the anomaly at a frequency of 500 MHz and in a field of 7 T does not vary significantly between 76 and 69 K. The data at 76 K were multiplied by a scale factor which was chosen such that the peaks of the two curves coincide.

tions from this scaling behavior.

Sound velocity data measured at a fixed temperature close to the superconducting transition at different frequencies can also roughly be superposed in a masterplot, however, even at 76 K there remain some small discrepancies at angles far away from the maximum. The peak amplitude as a function of frequency at this temperature is shown in Fig. 5.

We have also measured the field dependence of the anomaly at fixed angle and temperature values. At 4 K it is strictly quadratic. We have increased and decreased the field continuously and also in steps of one tesla. No significant relaxation was seen within the experimental accuracy. At 76 K it is difficult to determine the exact

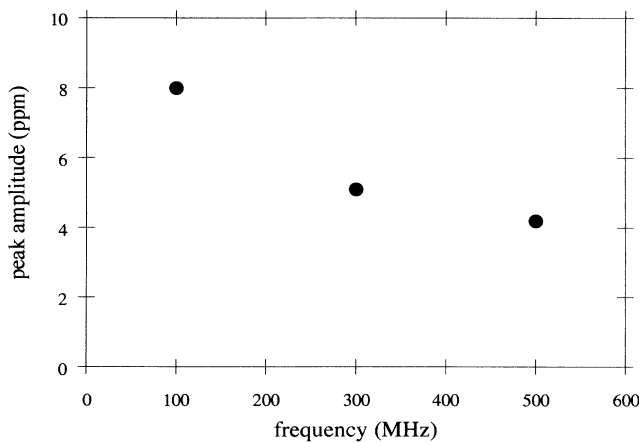


FIG. 5. Frequency dependence of the peak amplitude of the angular sound velocity anomaly at a temperature of 76 K and in a field of 7 T. As mentioned at the end of the experimental section, these data may have a global offset of several ppm.

field dependence because even at 7 T the variation is only a few ppm. The data suggest a dependence that is weaker than quadratic.

Finally, we have checked the dependence of the sound velocity variation on the amplitude of the surface waves. At low temperatures, no variation was detected within a dynamic range of 20 dB.

THEORY

We will start by discussing the general question of how the velocity of acoustic surface waves in a conducting and magnetic thin film is modified in the presence of a strong magnetic field. To our knowledge no quantitative analysis of this experimentally important configuration has been published up to now and it may be useful for a variety of thin film physics problems. In a second section we apply the general formulas to the particular problem of a thin HTC superconductor film.

There are two basic mechanisms that lead to magnetoelastic surface-wave effects in thin films. The first is due to the magnetization of the layer: if the material has a strong remanence or an anisotropic susceptibility the surface deformation due to the acoustic wave induces an oscillating stray field that will exert magnetic stress forces on the thin film; they contribute to the effective elastic constants and thus modify the Rayleigh velocity. The second mechanism is due to transport currents perpendicular to the sagittal plane; they are driven by Lorentz forces that act on the electrons in the layer when it is moved by the acoustic surface wave; the electromagnetic forces on these currents modify the acoustic surface-wave velocity. Throughout the discussion we will assume that the substrate on which the thin film is deposited is non-magnetic and isolating.

As a starting point of a quantitative analysis, it is useful to consider the perturbation of the electromagnetic field outside the layer whose thickness is taken to be much less than the acoustic wavelength. Figure 6 illustrates the coordinates we use. The symmetry of the experimental configuration only permits solutions of the form

$$\delta \mathbf{B} = (\alpha + \beta s) \begin{bmatrix} s \\ 0 \\ -i \end{bmatrix} \exp[skz + i(kx - \omega t)], \quad (1)$$

$$\delta \mathbf{E} = \frac{\omega}{k} (\alpha s + \beta) \begin{bmatrix} 0 \\ i \\ 0 \end{bmatrix} \exp[skz + i(kx - \omega t)].$$

The dimensionless parameter s is -1 in the upper and

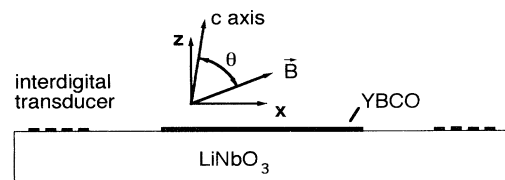


FIG. 6. Coordinates and angles used in the calculations.

1 in the lower half plane. In dielectric media its modulus is slightly smaller than one, but since the correction is given by the square of the ratio of the velocities of sound and light, it can safely be neglected. k is the wave vector and α and β are the complex amplitudes of the two possible modes. Nonzero amplitudes imply currents in the thin layer: the α mode is coupled to their component which is symmetric with respect to the reflection $z \rightarrow -z$, the β mode to the antisymmetric part. Since we are assuming that the acoustic wavelength is much larger than the layer thickness the latter contribution can be neglected.

We will now determine the mechanic stress T_{ij} on the layer due to the electromagnetic field. In particular we need its oscillating part δT_{ij} which contributes to the effective elastic constants that determine the acoustic surface-wave velocity. Using the Maxwell stress tensor we calculate the flow of momentum through a surface element due to electromagnetic fields and finally obtain

$$\begin{aligned} \delta T_{xz} &= -\frac{2\alpha B_z^0}{\mu_0} \exp[i(kx - \omega t)] , \\ \delta T_{zz} &= \frac{2\alpha B_x^0}{\mu_0} \exp[i(kx - \omega t)] . \end{aligned} \quad (2)$$

B^0 is the applied static magnetic field; higher-order terms in α have been neglected. The influence of an applied field on the velocity of elastic surface waves can now be calculated for a given α by taking account of the magnetic stress forces in the boundary conditions of the layer. Of course the forces are not really localized at the surfaces, but since we are considering very thin films, the resulting errors are negligible. To obtain the velocity v one has to superpose acoustic surface-wave solutions for the substrate and the layer that satisfy the various mechanic boundary conditions.⁸ This amounts to looking for the zeros of the coefficient determinant of a system of six linear equations. An exact solution of this problem requires a numeric calculation. We have written a program that uses standard methods⁸ and tested it by calculating the velocity of the surface waves in various thin metal layers on lithium niobate in the absence of magnetic fields. Results for these cases are available in the literature; they are in excellent agreement with those obtained with our program.

The problem of determining the Rayleigh wave velocity anomaly due to a thin conducting and magnetic film in the presence of a strong applied magnetic field has thus been reduced to the calculation of a single scalar parameter, the electromagnetic perturbation amplitude α defined in Eq. (1). As mentioned above it depends on the transport and magnetization currents in the layer. Since the magnetic field is taken to be in the xz plane and the electric field in the y direction the total oscillating current density must be of the form

$$\mathbf{j} = j_0 \exp[i(kx - \omega t)] \hat{\mathbf{y}} = -\frac{2\alpha}{\mu_0 h} \exp[i(kx - \omega t)] \hat{\mathbf{y}} \quad \text{for } |z| \leq h/2 . \quad (3)$$

In order to calculate α we have to determine \mathbf{j} in terms

of its physical origins:

$$\mathbf{j} = \sigma \mathbf{E} + \sigma (\mathbf{v} \times \mathbf{B}^0) + \frac{\nabla \times \delta \mathbf{M}}{\mu_0} . \quad (4)$$

The first two terms describe transport currents driven by electric fields: \mathbf{E} is associated with the α mode and given by Eq. (1). The second term is due to the additional field that arises when you transform \mathbf{B}^0 into the local frame of reference of the layer which is moved by the Rayleigh wave with velocity \mathbf{v} . The third term describes oscillating magnetization currents. It can be shown that in the approximation $kh \ll 1$ it reduces to $-2i\delta M_z/h$. To get a more explicit expression for the last term of Eq. (4) we determine the magnetization in a local frame of reference that is fixed with respect to the crystal axes at a given point of the thin film. The layer will "see" a periodic tilting of the applied field by a small angle $\delta\theta$. We rotate the resulting magnetization to the global frame which is fixed relative to the applied static field and subtract the static part:

$$\delta \mathbf{M} = \begin{bmatrix} 1 & 0 & -\delta\theta \\ 0 & 1 & 0 \\ \delta\theta & 0 & 1 \end{bmatrix} \left[\mathbf{M} + \frac{\partial \mathbf{M}}{\partial \theta} \delta\theta \right] - \mathbf{M} . \quad (5)$$

Using the following expression for the displacement $\delta \mathbf{r}$ of the layer by the Rayleigh wave:

$$\begin{aligned} \delta \mathbf{r} &= \begin{bmatrix} u_x \\ 0 \\ u_z \end{bmatrix} \exp[i(kx - \omega t)] , \\ \delta\theta &= iku_z \exp[i(kx - \omega t)] , \end{aligned} \quad (6)$$

and the three previous equations we finally obtain

$$\alpha = \frac{(-i\mu_0\sigma\omega h/2)(u_x B_z^0 - u_z B_x^0) - ku_z(M_x + \partial M_z/\partial\theta)}{1 + i\mu_0\sigma\omega h/2k} . \quad (7)$$

This general formula gives the electromagnetic field perturbation in terms of the conductivity and the magnetic properties of the thin film that is deformed by the acoustic surface wave. As mentioned above, the determination of the corresponding sound velocity change is straightforward but it requires a numeric calculation. However, some general features can be derived directly from Eq. (7): for conductivities that are much smaller or much larger than the "crossover value" $2k/\omega\mu_0 h$ there are two qualitatively different types of behavior. If σ is small α will be dominated by the magnetic properties of the film. However, if it has an isotropic magnetic susceptibility, the derivatives of M_z and M_x cancel and there is no magnetoelastic effect. Surface-wave measurements are thus directly sensitive to the anisotropy of the susceptibility of a magnetic layer. We will now discuss the opposite case where σ is much larger than the crossover value $k/\omega\mu_0 h$. Any flux change through the surface will then be screened off by transport currents and the magnetization contribution in Eq. (7) is suppressed. The forces that act on the surface become independent of the layer thick-

ness and also of the conductivity. Only in the vicinity of the crossover can the conductivity be obtained from surface-wave velocity data. If both transport and magnetization currents are present the quantitative analysis will generally be difficult but even in that case, the crossover itself can be used to estimate σ .

For the sake of completeness, we would like to mention that if the substrate is piezoelectric, the elastic surface wave induces an additional electric field that leads to currents in the films.⁹ However, these fields are in the sagittal plane and therefore do not couple to the modes described by Eq. (1).

Having outlined a general theory of magnetoelastic surface-wave effects in thin layers, we will now turn to the particular case of high- T_c superconductor films. Recent results of pinning theory provide an explicit expression for the rf conductivity in the presence of vortices:¹⁰

$$\sigma^{-1} = i\omega\mu_0 \left[\lambda_L^2 + \frac{B^2}{\mu_0 a_L} \frac{1-i/\omega\tau}{1+i\omega\tau_0} \right] \equiv i\omega\mu_0 \lambda_{ac}^2. \quad (8)$$

λ_L is the London penetration depth for fields that are parallel to the c axis, a_L the Labusch parameter, τ the relaxation time constant for vortices that move by thermally activated hopping, τ_0 the relaxation time constant for vortices that move by viscous relaxation, and λ_{ac} is the ac penetration depth. It describes the exponential decay of a small applied magnetic ac perturbation that penetrates into the surface of a superconductor in the presence of a strong static field. For a discussion of Eq. (8) we refer the reader to the literature.¹⁰ The above-mentioned criterion for the crossover to a material-independent behavior at high conductivities can in the present case be expressed in terms of three characteristic lengths: If the geometric mean of the layer thickness and the acoustic wavelength strongly exceeds λ_{ac} , the "universal" limiting case is reached. This will occur at low temperatures since the relaxation times and the Labusch parameter increase with falling temperature.² If in addition $\omega\tau_0 \ll 1$, which will be true at least for frequencies below 1 GHz according to experimental data of high- T_c superconductors,¹¹ the limiting case will first be reached at low frequencies. Numeric calculations for the case of an $\text{YBa}_2\text{Cu}_3\text{O}_7$ layer on LiNbO_3 show that in the "universal" limit the anomaly will essentially scale with B_x^2 . If the crossover to this characteristic behavior can clearly be identified in experimental data, it can be concluded that under these conditions $|\lambda_{ac}|^2 \approx 2k/h$.

At temperatures close to T_c and at high frequencies the ac penetration depth is much larger than the crossover value and the magnetization part of Eq. (7) becomes dominant. There are two contributions to the dynamic magnetization of a high- T_c superconductor: one is intrinsic because it is due to the anisotropy of the effective electronic mass, the other is caused by pinning and therefore strongly depends on the defects in the sample. For the intrinsic contribution we use the results obtained in the framework of the anisotropic London model.¹²

$$\mathbf{M} = \frac{-H^*}{4\pi\sqrt{m(\theta)}} \begin{bmatrix} m_1 \sin(\theta) \\ 0 \\ m_3 \cos(\theta) \end{bmatrix}, \quad H^* \equiv \frac{\phi_0 \ln(\eta B_{c2}/B)}{8\pi\mu_0 \langle \lambda_L \rangle^2}. \quad (9)$$

In this expression η is a constant of the order of unity that depends on the vortex lattice structure and $\langle \lambda_L \rangle$ the geometric mean of the London penetration depths in the a , b , and c directions. m_1 and m_3 are the effective electronic masses perpendicular and parallel to the c axis with a normalization $m_1^2 m_3 = 1$ and $m(\theta)$ is given by

$$m(\theta) = m_1 \sin^2(\theta) + m_3 \cos^2(\theta), \quad (10)$$

where θ is the angle between \mathbf{M} and the c axis. Before using these formulas we have to discuss to what extent they are valid in a thin film of $\text{YBa}_2\text{Cu}_3\text{O}_7$.

If the vortex lattice constant is much smaller than the film thickness very general arguments¹² show that for fields in the range $B_{c1} \ll B \ll B_{c2}$ the shape-dependent demagnetization field effects do not modify the magnetization significantly. However, this analysis does not take surface screening currents into account. More theoretical work is needed to resolve this problem, which is planned to be the subject of a forthcoming paper. A more fundamental question is to what extent the London model can be applied at temperatures far below T_c . Since the coherence length of the superconducting wave function becomes smaller than the CuO_2 layer separation below $0.9T_c$ (Ref. 13) the three-dimensional description of the anisotropy in terms of a mass tensor is no longer adequate at lower temperatures. Very recently, the magnetization of a layered superconductor has been calculated in the framework of the Lawrence-Doniach model.¹⁴ For magnetic fields that are accessible by conventional experimental techniques the corrections are predicted to be negligible in the case of $\text{YBa}_2\text{Cu}_3\text{O}_7$. We will therefore only consider the London approach, even though it does not provide a correct microscopic description of the vortices at low temperatures. Inserting Eq. (9) into (7) we get

$$\alpha = -\mu_0 \frac{m_1(m_1 - m_3)}{[m(\theta)]^{1.5}} \frac{H^*}{4\pi} \sin^3(\theta) k u_z. \quad (11)$$

Using the normalization condition for m_1 and m_3 it can easily be shown that the maximum of $\alpha(\theta)$ is proportional to $(m_3/m_1)^{5/6}$ so that large effects may be expected for very anisotropic materials such as $\text{Bi}_2\text{Sr}_2\text{CaCu}_2\text{O}_{8+x}$. The factor $(m_1 - m_3)$ clearly shows that for isotropic superconductors there is no field perturbation. The shape of the angular dependence of the resulting sound velocity anomaly for the normalized peak value depends only on m_3/m_1 and can therefore be used to extract this parameter from experimental data. Inserting Eq. (11) into (2) shows that the field dependence of the effect is linear. For $kh \ll 1$ the magnetic and the elastic forces have the same frequency dependence, therefore the sound velocity anomaly should be independent of frequency.

To identify the regime that is dominated by intrinsic

magnetization effects in experimental data, the following scaling test can be used.

Consider the angular sound velocity variation at two slightly different temperatures. The influence of pinning effects on magnetization and conductivity is negligible if the two curves differ just by a scale factor. The criterion works because the relevant pinning effects can be expressed as a function of the ac penetration depth which in turn depends on the quantity $\omega\tau$ which rapidly rises with falling temperature. Equation (8) shows that as soon as $\omega\tau$ has exceeded the value 1, a further increase will no longer have a strong influence on λ_{ac} . Experimental evidence clearly shows that the activated relaxation time τ has a strong angular dependence.¹ As a consequence, the form of the angular dependence of λ_{ac} and of all pinning-related sound velocity anomalies will change qualitatively with temperature.

If, on the other hand, the intrinsic magnetic anisotropy is dominant, no qualitative change of the angular variation is expected unless the effective masses vary with temperature or strong two-dimensional effects set in.

Of course the test will only work in a temperature region that is sufficiently close to T_c so that $\omega\tau$ will not yet be larger than one in the entire angular range.

DISCUSSION

As can be seen in Fig. 1, there is a sharply peaked magnetoelastic sound velocity anomaly at $0.9T_c$. Its maximum coincides with the direction of the CuO_2 planes which are not parallel to the surface in our sample. This clearly shows the intrinsic nature of the effect which is not directly linked to the sample geometry. The continuous line is a fit that has been calculated using the London model and the formalism described in the preceding section. To make sure that effects that are related to pinning do not contribute we have superposed data measured at temperatures of 76 and 69 K and a frequency of 500 MHz in the masterplot shown in Fig. 4. The reasonable agreement confirms the intrinsic nature of the effect. Below 300 MHz, it is no longer possible to obtain a masterplot down to 69 K. This is in agreement with theory because below the thermally activated flux flow transition the term that contains the ac penetration depth in the denominator of Eq. (7) rises with falling frequency. Thus there is substantial evidence that at least the data measured at 76 K and above 100 MHz are dominated by the intrinsic magnetization effect described in the preceding section. The ratio of effective masses obtained from the fit shown in Fig. 1 is 23 with an uncertainty of 4 which is in agreement with magnetization¹⁵ and some recent torque magnetometry data¹⁶ as can be seen in Table I.

Strictly speaking the anisotropic London model cannot be used for $\text{YBa}_2\text{Cu}_3\text{O}_7$ at $0.9T_c$ which corresponds to 76 K for our sample because at this temperature, the coherence length is comparable to the layer spacing. The fact that we will obtain a reasonable fit with an anisotropic mass model is in agreement with the calculations in the framework of the Lawrence-Doniach model mentioned in the preceding section and also with H_{c1} measurements¹¹

TABLE I. Ratios of effective electronic masses parallel and perpendicular to the CuO_2 planes of $\text{YBa}_2\text{Cu}_3\text{O}_7$ obtained by different methods.

Method	m_3/m_1	Reference
Measurement of H_{c1}		
via rf penetration depth	11.6	[11]
Measurement of H_{c2}	28	[17]
Torque magnetometry	60	[13]
Torque magnetometry	22.5–27.5	[16]
Direct measurement of the magnetization	25–35	[15]
Surface acoustic wave velocity anisotropy	19–27	This paper

which are compatible with a mass ratio that is constant down to low temperatures. On the other hand, Farrel *et al.*¹³ have reported torque measurements that show deviations from anisotropic London theory below $0.9T_c$ at small angles between the CuO_2 layers and the applied field. However, since these data were measured far below the irreversibility line it is not entirely clear to what extent they are influenced by pinning effects. As the scaling test mentioned above strongly supports the hypothesis that our data at $0.9T_c$ are determined by the intrinsic magnetization effect, it is interesting to perform a detailed comparison with the torque magnetometry results. We have therefore fitted the data for angles more than 8° away from the orientation that corresponds to the sound velocity peak with our calculations that are based on the anisotropic London model. Figure 7 shows the resulting curve together with the previously excluded data. The measured peak is sharper than the curve obtained from the London model fit, it even suggests a cusp. In agreement with this general trend the mass ratios obtained by fitting data close to the peak are significantly larger than those obtained at larger angles. Analogous deviations from anisotropic London theory have been observed by Farrel *et al.*¹³ Before trying to analyze the discrepancy

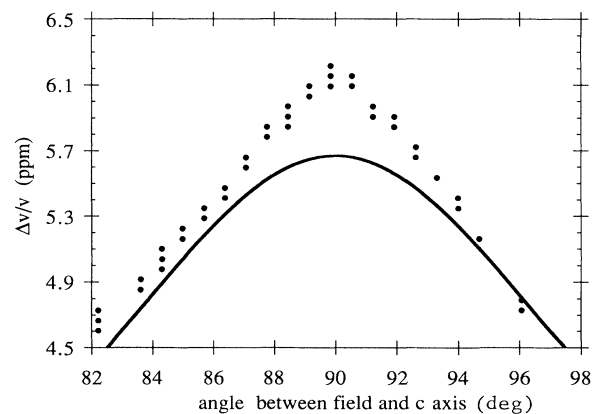


FIG. 7. High prediction data at a temperature of 76 K and a frequency of 500 MHz. The field strength was 7 T. The continuous line corresponds to a fit that has been obtained with the anisotropic London model by excluding data in the angular range shown in the figure.

using the Lawrence-Doniach model we think that it would be very helpful to perform a series of measurements on samples with decreasing oxygen content. The resulting successive increase of the anisotropy should clearly reveal increasing deviations from London theory. The thin film geometry is particularly favorable for this kind of study and indeed, we are planning such an experiment.

Figure 2 shows that as expected the amplitude of the magnetoelastic anisotropy effect rapidly increases with falling temperature. At $0.8T_c$ the slope abruptly changes and at the same time an effect that scales with B_x^2 sets in. This is in excellent qualitative agreement with our prediction: the phenomenon corresponds to the crossover where the ac penetration depth becomes smaller than the geometric mean of the layer thickness and the acoustic wavelength. Using the formulas of the preceding section we conclude that the Labusch parameter at $0.8T_c$ and 7 T is 5×10^{21} N/m⁴. Wu and Sridhar¹¹ have obtained a force constant per vortex of about 3×10^4 N/m² by means of a rf penetration depth measurement on a single crystal at 10^{-2} T. Using the empirical relation $a_L \propto B^2$ (Ref. 1) this corresponds to a Labusch parameter which is about one order of magnitude larger than our result. Since the exponent of the scaling law is not known very precisely, there is no significant difference between the results obtained by the two methods. This is interesting because critical currents J_c measured on thin films are systematically higher than those obtained for bulk samples. The relation $a_L s_p = BJ_c$,¹ where s_p is the range of the pinning potential, suggests that the range of the potential and not its attractive force are the origin of the different critical currents. However, before drawing such a conclusion the critical current of our films has to be checked. Furthermore very recent results of pinning theory¹⁰ show that the analysis used in Ref. 11 which does not take into account the influence of image vortices and the nonlocal elasticity of the vortex lattice may have to be reconsidered. A comparison with vibrating reed measurements of the Labusch constant at fields comparable to those used in our experiment would be very interesting, but we are not aware of any such data for YBa₂Cu₃O₇. The Labusch parameter obtained for a slightly oxygen deficient 1:2:3 superconductor¹ is much lower than the ones we have obtained.

The anomaly that we have measured at a temperature of 5 K and a frequency of 100 MHz scales with B_x^2 , which

is in excellent agreement with the predictions derived from Eq. (3). As explained in the theory section, this limiting behavior is interesting because it confirms our analysis, but it does not give any additional information about the properties of YBa₂Cu₃O₇.

Thus we have shown that a measurement of the angular dependence of the velocity of Rayleigh waves in a thin superconducting film gives information about the anisotropy of the rf penetration depth and the intrinsic anisotropy of the magnetization. Compared to other methods, the new technique has the advantage that for small Labusch parameters and at sufficiently high frequencies it can give access to the intrinsic magnetization far below the depinning line. Another important point is that it can be used to investigate thin film samples which allow a rapid and homogeneous change of the oxygen content. Multilayer materials whose magnetic anisotropy is very interesting are available only in this form.

CONCLUSIONS

We have presented a general theory of magnetoelastic surface-wave effects in thin films which can be used to extract the rf conductivity and the magnetic properties of the sample from experimental data. By applying it to our measurements of the Rayleigh wave velocity of thin YBa₂Cu₃O₇ films in the presence of a strong magnetic field of variable orientation, we have obtained the anisotropy of the effective electronic mass and the value of the Labusch parameter at $0.8T_c$. A detailed analysis has revealed small but systematic deviations from the anisotropic London model which confirm earlier results that were obtained by torque magnetometry.¹³ The anomaly can be explained qualitatively by a crossover from 3D to 2D vortices. By means of a scaling test we have shown that in our experiment pinning effects can be ruled out. However, more theoretical and experimental work is needed to understand clearly the influence of the thin film geometry on the vortex lattice and the dimensional crossover of the vortices.

ACKNOWLEDGMENTS

We would like to thank M. Coignard of the Institut d'Electronique Fondamentale in Orsay who deposited the interdigital transducers and D. Guggi of the Forschungszentrum Jülich who performed the x-ray measurements.

¹A review is given in P. Esquinazi, *J. Low Temp. Phys.* **85**, 139 (1991).

²J. Pankert, G. Marbach, A. Comberg, P. Lemmens, P. Frönig, and S. Ewert, *Phys. Rev. Lett.* **65**, 3052 (1990).

³H. P. Baum, Ph.D. thesis, University of Wisconsin, Milwaukee, 1990.

⁴S. Lee, C. Chi, G. Koren, and A. Gupta, *Phys. Rev. B* **43**, 5459 (1991).

⁵M. Saint-Paul, F. Pourtier, B. Pannetier, J. C. Villegier, and R. Nava, *Physica C* **183**, 257 (1992).

⁶T. Venkatesan, C. C. Chang, D. Dijkkamp, S. B. Ogale, E. W. Chase, L. A. Farrow, D. M. Hwang, P. F. Miceli, S. A. Schwarz, J. M. Tarascon, X. D. Wu, and A. Inam, *J. Appl. Phys.* **63**, 4591 (1988).

⁷A. Höhler, *Appl. Phys. Lett.* **54**, 1066 (1989).

⁸G. W. Farnell, and E. L. Adler, *Physical Acoustics IX*, edited by W. P. Mason and R. N. Thurston (Academic, New York, 1976).

⁹R. Adler, *IEEE Trans. Sonics Ultrason.* **SU-18**, 3 (1971).

¹⁰E. H. Brandt, *Phys. Rev. Lett.* **67**, 2219 (1991).

¹¹D. Wu and S. Sridhar, *Phys. Rev. Lett.* **65**, 2074 (1990).

¹²V. G. Kogan, *Phys. Rev. B* **38**, 7049 (1988).

¹³D. E. Farrell, J. P. Rice, D. M. Ginsberg, and J. Z. Liu, *Phys. Rev. Lett.* **64**, 1573 (1990).

¹⁴D. Feinberg, *Physica C* **194**, 126 (1992).

¹⁵M. Tuominen, A. M. Goldmann, Y. Chang, and P. Jiang,

Phys. Rev. B **42**, 412 (1990).

¹⁶B. Janossy, D. Prost, S. Pekker, and L. Fruchter, *Physica C* **181**, 51 (1991).

¹⁷U. Welp, W. K. Kwok, G. W. Crabtree, K. G. Vandervoort, and J. Z. Liu, *Phys. Rev. Lett.* **62**, 1908 (1989).